ISTANBUL TECHNICAL UNIVERSITY ★ EARTHQUAKE ENGINEERING AND DISASTER MANAGEMENT INSTITUTE

THE RESPONSE OF UNREINFORCED MASONRY TO LOW-AMPLITUDE RECURCIVE LOADS: CASE OF GRONINGEN GAS FIELD

M.Sc. THESIS

Dimitrios DAIS

Earthquake Engineering and Disaster Management

Earthquake Engineering Programme

MAY 2017

ISTANBUL TECHNICAL UNIVERSITY ★ EARTHQUAKE ENGINEERING AND DISASTER MANAGEMENT INSTITUTE

THE RESPONSE OF UNREINFORCED MASONRY TO LOW-AMPLITUDE RECURCIVE LOADS: CASE OF GRONINGEN GAS FIELD

M.Sc. THESIS

Dimitrios DAIS
(802151206)

Earthquake Engineering and Disaster Management

Earthquake Engineering Programme

Thesis Advisor: Assistant Prof. Dr. Ihsan Engin Bal

MAY 2017

Dimitrios Dais, a **M.Sc.** student of ITU **Institute of Earthquake Engineering and Disaster Management** student ID 802151206, successfully defended the **thesis** entitled "**THE RESPONSE OF UNREINFORCED MASONRY TO LOW-AMPLITUDE RECURCIVE LOADS: CASE OF GRONINGEN GAS FIELD**", which he prepared after fulfilling the requirements specified in the associated legislations, before the jury whose signatures are below.

Thesis Advisor :	**Asst. Prof. Dr. Ihsan Engin BAL** İstanbul Technical University	.....
Jury Members :	**Asst Prof. Dr. Fatih SÜTÇÜ** İstanbul Technical University	.....
	Asst Prof. Dr. Hasan ÖZKAYNAK İstanbul Technical University	.....

Date of Submission : 5 May 2017
Date of Defense : 6 June 2017

ACKNOWLEDGEMENTS

Reaching the end of my Master's Thesis I feel thankful for having the opportunity to be supervised by my advisor, Assistant Professor Ihsan Engin Bal.
A special mention is reserved for Dra Eleni Smyrou for her contribution during the whole period of my Master Studies.
This work and the relevant US visit was financially supported by Istanbul Technical University within the "ITU – Researcher Education & Training Program ITU-AYP-2016", for a project titled "Investigation of the human caused earthquakes generated during the production of shale gas", with the contract number "ITU-AYP-2016-18". Their generous contribution is gratefully acknowledged.

May 2017 Dimitrios DAIS

Page

ABBREVIATIONS

bcm	**:** billion cubic meters
GIIP	**:** Gas Initially In Place
KNMI	**:** Koninklijk Nederlands Meteorologisch Instituut
NAM	**:** Nederlandse Aardolie Maatschappij
PGA	**:** Peak Ground Acceleration
PGV	**:** Peak Ground Velocity
URM	**:** Unreinforced Masonry

LIST OF TABLES

Page

LIST OF FIGURES

Page

THE RESPONSE OF UNREINFORCED MASONRY TO LOW-AMPLITUDE RECURCIVE LOADS: CASE OF GRONINGEN GAS FIELD

SUMMARY

Unreinforced masonry (URM) is a fragile material that responds to cyclic load reversals in a non-ductile way, unless special measures are taken. Damage occurs in large amplitude loads causing partial or total collapse in some cases, as it was observed in the past earthquakes. Response of URM to recursive, frequent but low-amplitude seismic loads, on the other hand, is a relatively new topic that needs experimental and analytical validation. This paper focuses on Groningen URM buildings that have been subjected to low-amplitude load reversals in the last decades, especially in the very last decade, due to the induced seismicity caused by gas extraction. In the paper, previous experimental findings are reviewed mostly focusing on the range of low amplitudes. An exercise with existing hysteresis rules, trying to find residuals after recursive seismic actions, has been presented.

1. INDUCED SEISMICITY - LITERATURE REVIEW

Induced seismicity accounts for mostly minor quakes and tremors which are triggered by human activities that change the stresses and strains on the Earth's crust. This human activity causes a rate of energy release which is unexpectedly high given the common level of historical seismic rate. This alteration of the seismicity rates might be expressed as an increase in the annual events and in the recorded magnitudes as well. The majority of the induced seismic events are of low magnitude. Nevertheless, some places experience on a regular basis larger seismic excitations, such as the Geysers geothermal plant in California which in average is being hit by two M4 events and 15 M3 events per year from 2004 to 2009. Another interesting example of the induced seismicity si the 2011 Oklahoma earthquake which was of the quite high magnitude of Mw = 5.7. Significant events that occurred all over the globe attributed to induced seismicity caused by various human activities are presented in the **Figure 1.1**. In the **Figure 1.2** a comparison of the seismicity rates between the Stillwater (Oklahoma) and San Francisco (California) is illustrated. As it can be inferred from the aforementioned figure, in early 2014 Oklahoma actually surpassed the San Francisco region, famous for its seismic excitations, in terms of the rate of earthquakes. It has to be noted that the Oklahoma region is lacking of any important fault and its seismic activity falls in the induced quakes category. This observation justifies the rising concern that has been risen especially the last years about the induced seismicity.

Regarding the causes of induced seismicity, there are several types of underground activities that may play role. Scientists have observed various human activities which induce the seismicity of a region such as the creation of artificial lakes, mining, waste disposal wells, hydrocarbon extraction and storage, groundwater extraction, geothermal energy and hydraulic fracturing.

One of the most common causes, however, is the exploitation of land gas fields. According to recent studies (Mulders, 2003) **[1]**, there is no doubt that the extraction of natural gas strongly influences the balance of forces in the reservoir layers. A view of a typical machinery used for the extraction of the natural gas is shown in the **Figure**

1.3. Specifically, induced seismicity in oil and gas extraction was firstly noticed in the 1930s. The most popular early case was in Wilmington of California where oil production caused a bunch of destructive quakes. In this case, the reason of the seismicity was assumed to be the subsidence arising from the rapid extraction of oil with replacing the extracted fluids. In order to mitigate the induced seismicity, the oil extraction was being replaced by water injections. This practice became very common in the oil and gas industry and in the recent years the injection of liquids under high pressure was utilized.

In cases where injected water induces seismic excitations of larger magnitudes, the excitations are most probably the outcome of reactivation of adjacent pre-existing faults by altering the subsurface pressure regimes that preserve the fault inactive. Invented in 1947, hydraulic fracturing, or fracking, is a method that facilitates the extraction of oil and gas from wells by increasing the number of fractures in the Earth's crust through which oil and gas can flow, and expanding the reach of fluid pathways (fractures), between the crust and the well. Injecting water, with some specific chemicals, at high pressure into low-permeability, or tight, rocks, fractures the rocks or stimulates slip across pre-existing faults and fractures, allowing for more oil and gas to be accessed by the well. A propping agent, usually sand particles, is also injected to keep the new fractures open.

Fracking takes a few hours to a few days, followed by a period where the fracking fluid is allowed to flow back to the surface where it is collected for disposal, treatment, or reuse. It is the disposal of this fluid, along with other waste and produced waters, by injection into deep wells that causes the earthquakes.

The injected fluids change the subsurface dynamics of pressure and friction, allowing things to move that would not ordinarily move or that would not move so often. The water is injected into a different rock formation than where the oil or gas is, usually, below the production zone.

Fracking itself, and subsequent enhanced recovery operations, inject water into rocks where oil or gas is being removed or where they have already been removed, which does not increase the pressure that much. However, water injection wells usually inject into pristine rocks, so injection increases pressures much more and makes induced earthquakes more likely. Where there are faults, the increased fluid pressure can push

back against the pressure holding the fault closed, thereby allowing the fault to move. The effects that fluid injection and withdrawal can have on nearby faults and have the potential to cause induced seismicity are presented schematically in the **Figure 1.4**.

Since water disposal wells typically operate for much longer times than the extraction wells, they tend to inject much more fluid than the fracking or drilling operations. Injections which are responsible for earthquakes above magnitude 3 involve hundreds of thousands of barrels injected fluids (or extracted fluids) cause earthquakes by changing the stress conditions on and within faults, bringing these stresses into a condition in which driving stresses equal or exceed resistive stresses, thereby promoting slip on the fault.

Induced seismicity usually is confined to the shallow part of the earth's crust, often in the vicinity of the formation where the injection is occurring. For example, while natural earthquakes in the central and eastern United States can occur at maximum depths of 25 to 30 km, the majority of potentially induced earthquakes in Oklahoma are occurring in the top 6 km, well into the shallow crystalline basement (McNamara et al., 2015) **[2]**. This shallow depth often explains why induced earthquakes as small as M 2.0 can be felt. In general, natural earthquakes occurring in the central and eastern United States are not felt at that low a level of magnitude unless they are very shallow. In **Figure 1.5** the typical seismic event impact that corresponds to each magnitude on Richter Scale is presented. It can be easily noticed that quakes of low magnitude normally cannot be perceived by humans, but as it was clarified above the induced events do not comply with this statement.

Human concern and anxiety has been created by these low-level ground shakings. Especially the injection-inducted seismicity even though is generally of a small magnitude and short duration, human anxiety has arisen given the very high rates of seismicity that characterize normally the induced events.

Due to the problems that have been described above, many states are now regulating wastewater injection in an effort to limit the risk of earthquakes **[3]**. Simultaneously, in the States there is an attempt to include in the updated Seismic Hazard Maps the seismic events deriving from the human activities (Petersen, M. D. et al., 2015) **[4]**.

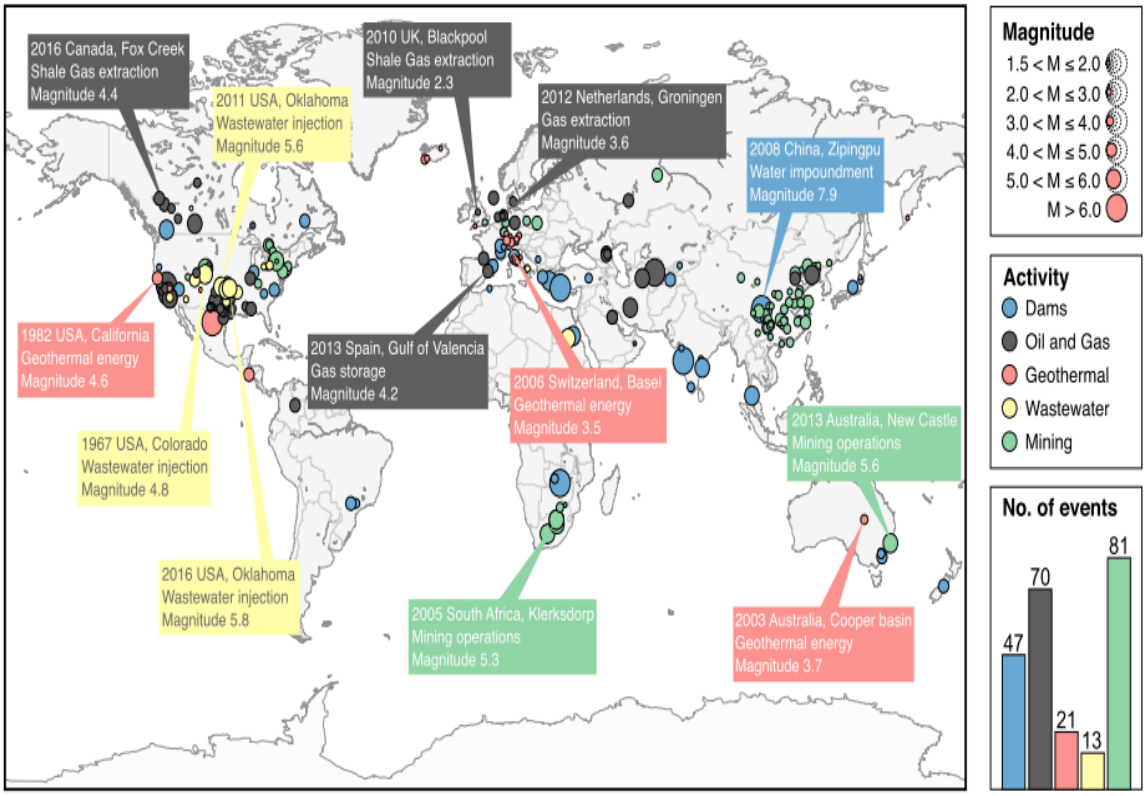

Figure 1.1: Significant events that occurred all over the globe attributed to induced seismicity caused by various human activities.

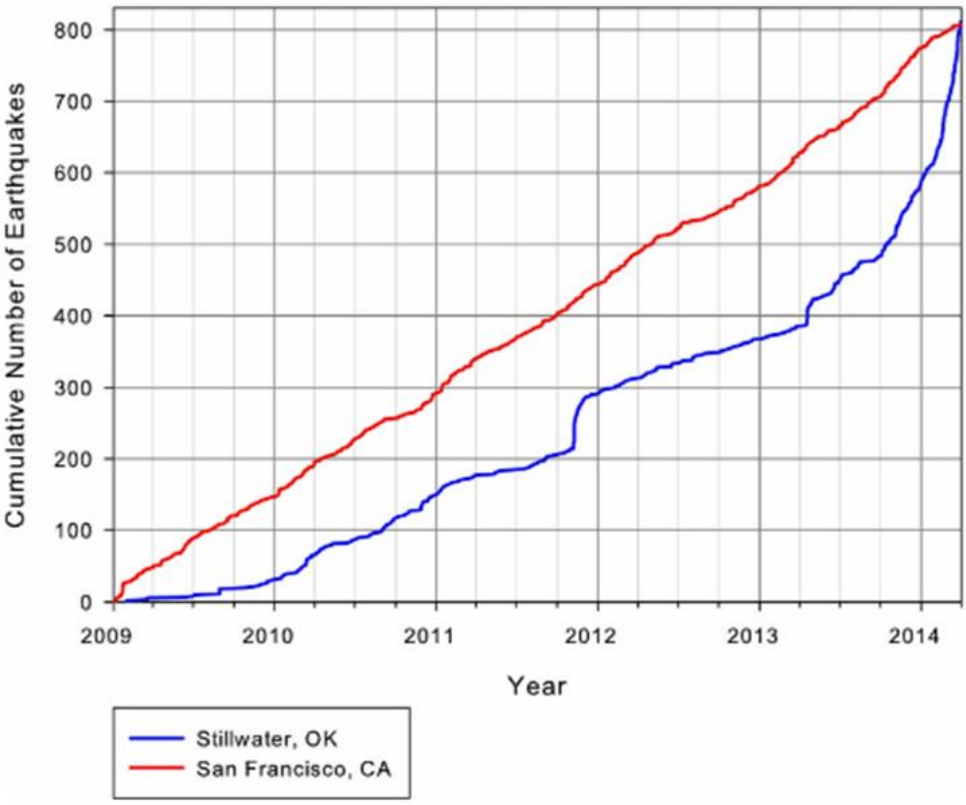

Figure 1.2: The Cumulative Number of Earthquakes for the Oklahoma region and a similarly sized area surrounding San Francisco given for the period 2009 - 2014.

Figure 1.3: A view of a typical machinery used for the extraction of the natural gas.

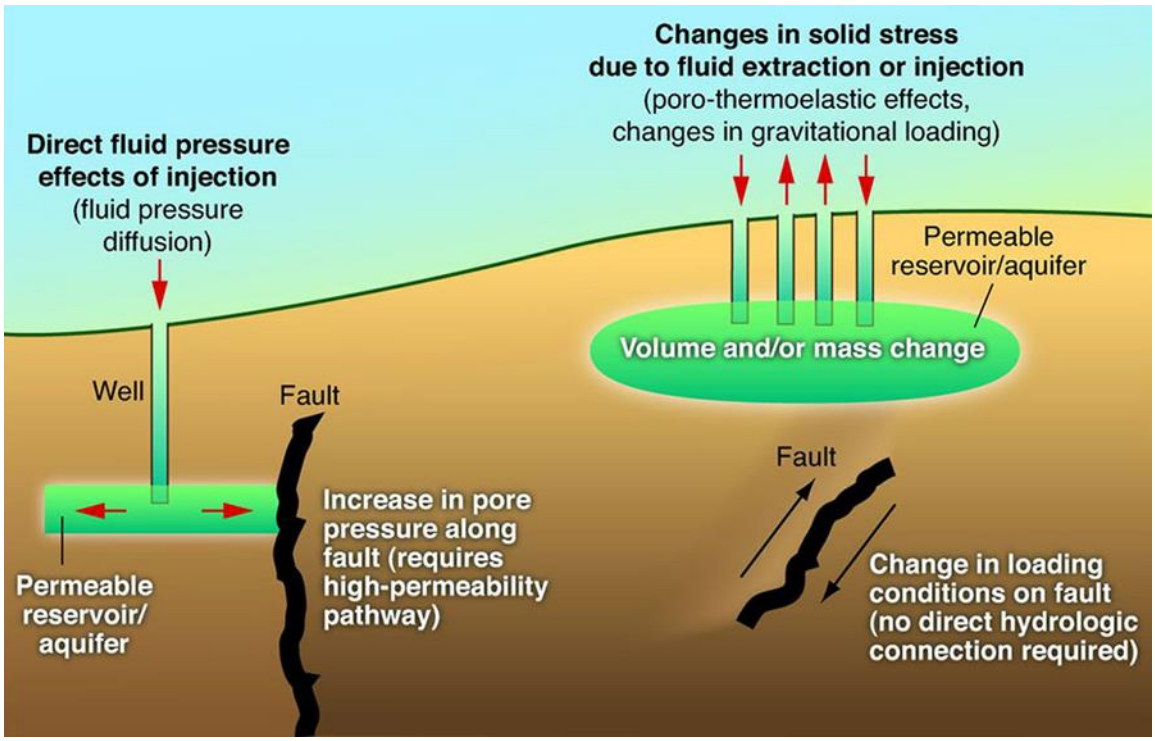

Figure 1.4: The effects that fluid injection and withdrawal can have on nearby faults and have the potential to cause induced seismicity.

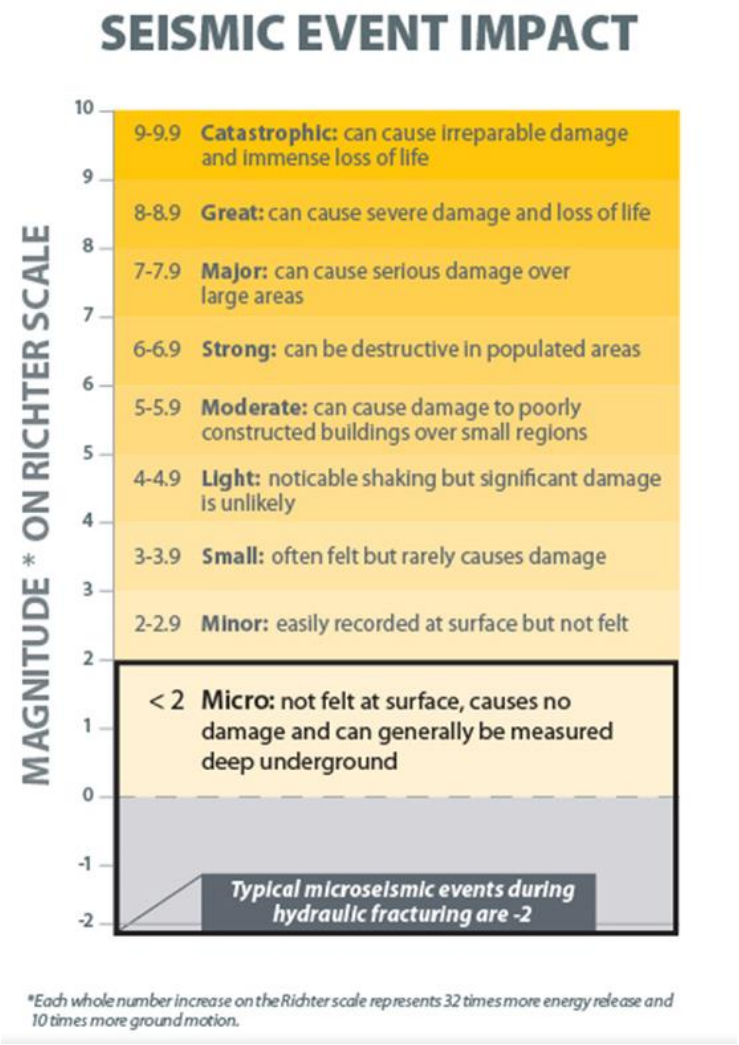

Figure 1.5: Typical Seismic Event Impact that corresponds to each Magnitude on Richter Scale.

2. GRONINGEN GAS FIELD

Groningen, located in the northeastern part of the Netherlands, is the largest gas field in Europe and 10th in the world. There has been extensive gas extraction taking place in the region and there are relatively "larger" magnitude induced earthquakes especially in the very last decade.

In the case of seismic events, the stress disturbances that occur during an earthquake are primarily due to natural tectonic processes. In the case of induced seismicity, however, the stress perturbations that are released during an earthquake are majorly due to human activities, as in the case of Groningen. In this case, the human activities do not directly aim to trigger an earthquake, however the changes in stress levels in rock layers trigger relatively small but repetitive earthquakes in non-seismic zones. The Groningen gas field is located in an area that is assumed as non-seismic, meaning that the seismic events apart from the induced seismicity, are inexistent. Interestingly enough, no earthquakes were reported from the Groningen area prior to 1991. This can be explained by the assumption that the events were smaller than the humanly perceptible levels.

Around 220 earthquakes with magnitude greater or even to 1.5 were registered in the period from 1991 till July 2013 in the Groningen area. In **Figure 2.1(a)** the epicenters of the seismic events between 2003 and 2016 in the area can be seen. Distribution of the events in terms of magnitude ranges can be seen in **Figure 2.1(b)**. A sudden increase in seismic events between 2011 and 2013 can clearly be observed in that figure. A threshold value of magnitude $M \geq 1{,}5$, makes 1996 the first year with a complete dataset. This threshold was imposed by KNMI in order to filter the earthquake data and avoid interference from network changes. **Figure 2.2** shows the annual number of earthquakes and the corresponding gas production. From this we conclude that on average the annual number of earthquakes has been increasing since 2003. A comparison can also be made between gas production and the number of earthquakes.

In **Figure 2.3**, the seismic zonation map of the Netherlands is given in accordance with the Eurocode-8. Particularly, the region of Groningen is classified as Seismic Zone A, which corresponds to PGA 9.81 cm/s^2 (0.01 g). This value was exceeded by far during the strong ground motion that was recorded at the Huizinge event on the 16th of August

2012 (Middelstum station). This observation makes evident the impact that the effect of induced seismicity on the area province of Groningen gas field. The seismicity of the region has been utterly changed; from non-perceived from the human it has turned into a quite destructive phenomenon.

The Groningen gas field, in the northeastern part of the Netherlands, is the largest gas field in Western Europe, with gas initially in place (GIIP) of close to 3000 billion m3 (bcm). The field was discovered in 1959 with the drilling of the Slochteren-1 well. From the start of production in 1963 through January 2015, 2115 bcm (75% of the GIIP) had been produced. The field is still a major supplier of natural gas to the northwestern European gas market. The production of gas leads to a decrease of the pressure in the reservoir, which is regarded to be the largest driving force behind the earthquakes. The first earthquake ($M \geq 1.5$) was observed at a cumulative production of around 1300 bcm. A slight increase of the slope is visible at a production of around 1700 bcm. In January 2014, it was decided to limit gas production in the central and highest-subsidence part of Groningen field and allow more production from the less compacted field periphery. More important, the production for five clusters of wells in the center of the field, corresponding to high compaction values, was limited to 3 bcm per year. Seismicity observed in 2014 was markedly different from that in earlier years. There appears to be a close link between induced seismicity and reservoir compaction resulting from extraction of gas. Because compaction manifests itself as surface subsidence, accuracy of the subsidence measurements is deemed much more important than previously thought. Although not yet statistically significant, this observation suggests a close link among production, compaction and seismicity. The mechanism behind the earthquakes is now generally considered to be (differential) compaction at reservoir level reactivating offset faults as originally proposed by (Roest and Kuilman, 1994) **[5]**. **Figure 2.4** shows an evident correlation between the epicenter of the quakes and the spatial distribution of the compactions that have been taken place due to the gas extraction **[6]**.

In order to mitigate both the effect of subsidence and induced seismicity and to increase the societal acceptances of these industrial activities, the Dutch government decided to move the gas production from the central part of the main field towards the less compacted peripheral parts of the Groningen field and to further reduce the overall production.

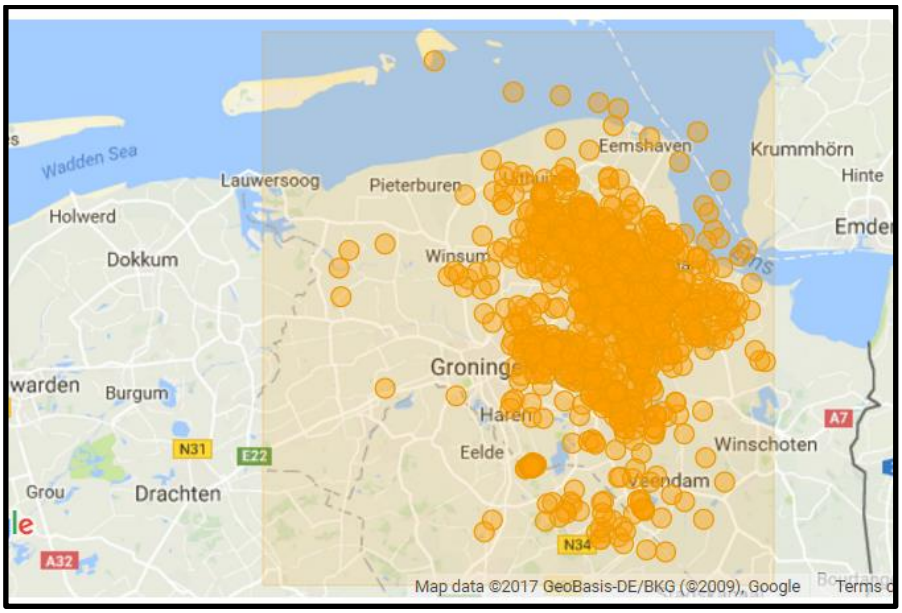

(a)

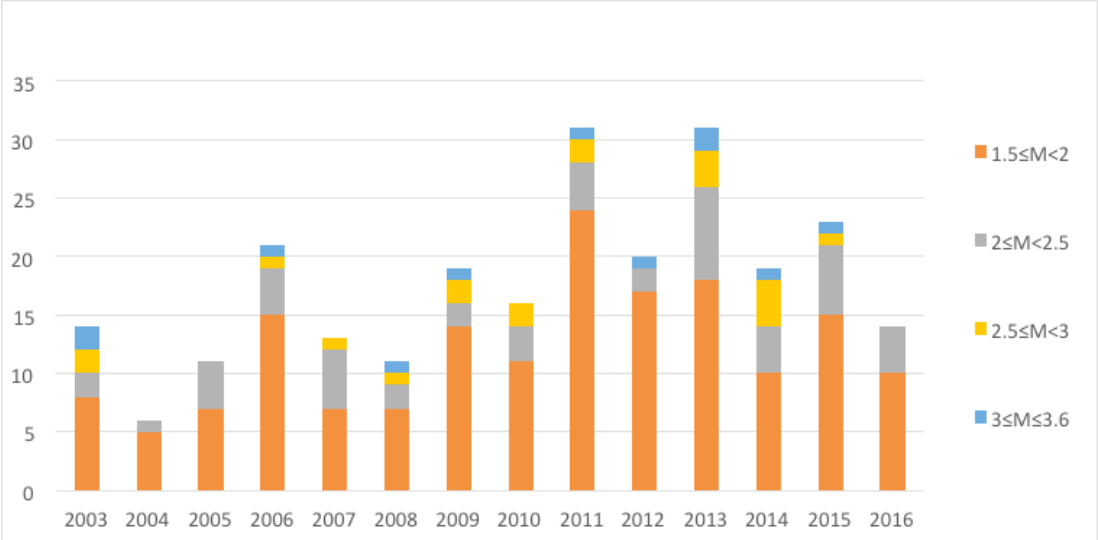

(b)

Figure 2.1: (a) The seismic events obtained from the KNMI Seismic Database for the Groningen region for the time period between 2003 – 2016 and **(b)** the distribution of the seismic events in a year basis for Magnitude 1.5+.

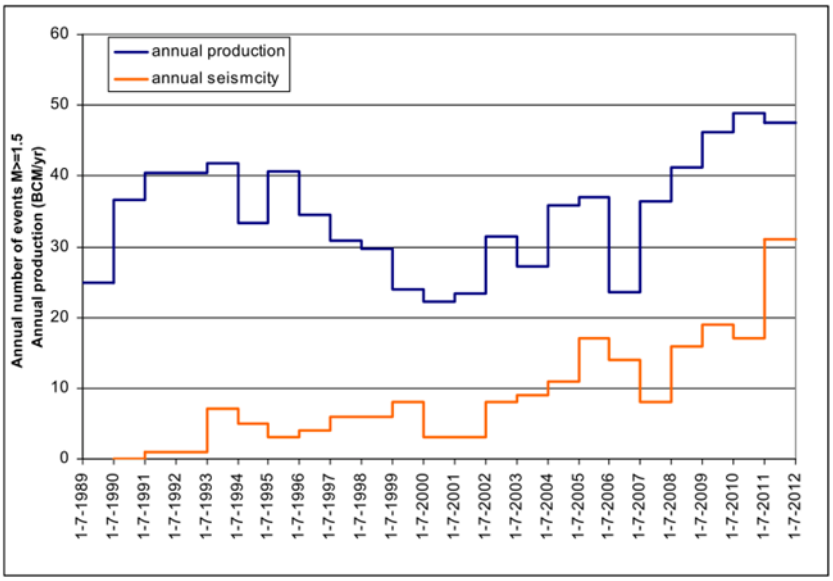

Figure 2.2: The annual gas production and the annual number of Earthquakes with magnitude 1.5 or higher are shown for the time period 1989 – 2012.

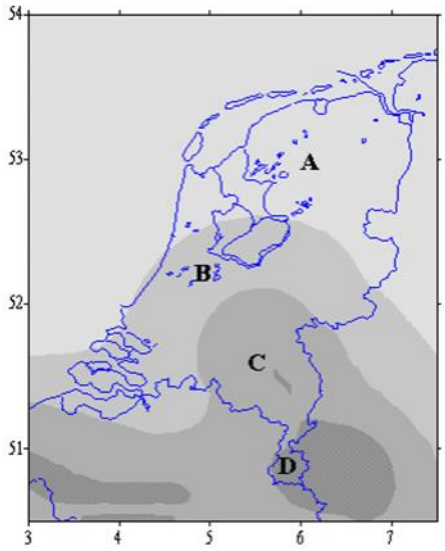

Figure 2.3: The seismic zonation map of the Netherlands is based on a seismic hazard study with a 10% of exceedance in 50 years (return period 475 years, and A means 0.01g PGA).

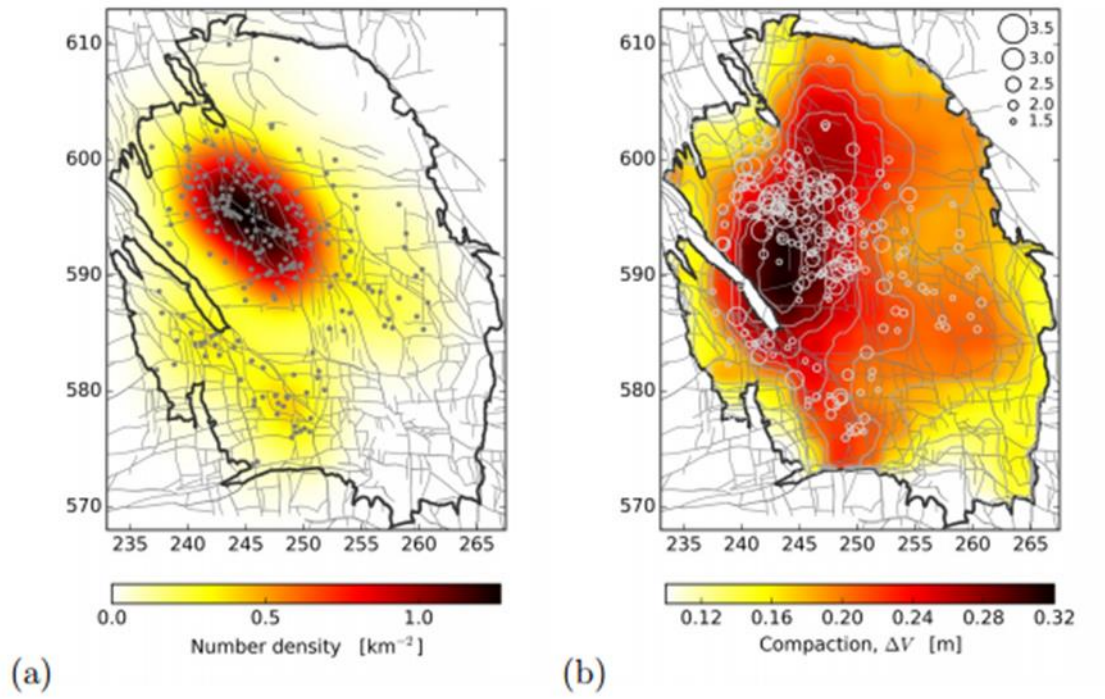

Figure 2.4: (a) Observed epicenters of ML greater or equal to 1.5 from 1995 to 2015. The underlying event number density function was estimated using the Gaussian kernel density method. **(b)** The same epicenters shown in respect to reservoir compaction estimated by inversion of the geodetic levelling data (Bierman et al., 2015) **[7]**.

3. CASE STUDY - DEFICIENCIES OF THE GRONINGEN REGION

This part of the current study will try to explain the main features that make the Groningen case so complicated and arouses the concern of the scientists. A paradox that ought to be analyzed is the fact that despite the magnitude of the seismic events is not very high they are proven to be quite destructive.

Firstly, a closer insight of typical structures that someone can come across in the region of Groningen could be quite indicative of the current situation. The single-story or two-story houses compose the main building stock in the region. The houses there are mostly made of unreinforced masonry (URM), traditionally without considering any seismic action into account because of the inexistence of such phenomena previously in the area. Low normal stresses on the load bearing and veneer walls, as well as the recursive nature of the seismic actions, despite their low amplitude, raise the question of whether micro damages accumulate during years of seismic actions. There is a limited experimental research on the low-cycle fatigue of masonry under recursive loads, but these are tests that were conducted for normal stresses **[8, 9]**. It was found in the previous research that there is development of micro cracks, and thus there is accumulation of damage in case of low amplitude loading in recursive fashion.

This complicated issue requires tiresome numerical but mostly experimental validation. This study, however, focuses mostly on, by using available experimental data, the URM response in low-amplitude range, as well as requirements of a compatible hysteresis model that can accurately represent both low- and high-amplitude regions of the force-deformation response.

The shallow depth of the induced earthquakes is leading to a limited area that is affected, but has the potential to attain very high intensity. As explained in previous chapter, shallow quakes arising from induced seismicity release more energy to the surface than natural deep quakes of the same magnitude. The structures in question, in Northern and Central Europe, are extremely prone to such events. Firstly, the aforementioned regions were considered to be aseismic from a natural perspective.

During the Huizinge event at 2012, which will be further investigated below, the PGA value prescribed from the local Seismic Codes was exceeded by far. The exceedance of the design capacity of the structures in combination with the lack of aseismic provisions puts them at great risk.

Moreover, the nature of these structures (low-rise and stiff) leads to quite short fundamental periods, matching with the dominant periods of the induced seismicity events. Another weak characteristic of these structures is the very low normal stress on the bearing walls resulting to remarkably small shear strength. Another destructive feature of the induced seismicity is the extremely high seismicity rates, even if the recorded magnitudes are pretty low. There is a significant accumulation of energy dissipation translated to minor but accumulating damages in the structural members of the buildings that finally leads to important damage especially when the relatively strong ground motion strikes.

Emphasis has to be given to the soil condition of the Groningen region. The soil in the seismic zone consists of soft clay. The clay behaves like a giant rubber band and has the potential of aggravating the quakes. This is called resonant rise. Furthermore, the geological profile of the region deteriorates the impact of the earthquakes. Dense urban development can dampen a quake. Whereas, in the empty countryside, like in the case of Groningen, a ground motion can spread with resonant rise until it reaches an urban environment. At this point it is highlighted that compared to gas fields in other parts of the world, the Groningen gas field is densely populated and the seismic events are in this case are affecting a wide range of urban complexes and their inhabitants.

4. DAMAGES - CURRENT CONDITION

As a matter of fact, at the under-investigation region of Groningen structures being retained by shore-up walls is a very common sight nowadays that the phenomenon of the high seismicity rates is taking place in a wide extent. **Figure 4.1** presents typical houses and other structures of the region which currently are under immense need of repairs and possible actions of retrofitting them is considered of paramount importance. Another side effect of the current situation in Groningen has to do with the economical aspect of the problem. The house owners are complaining that the value of their properties has drastically decrease during the last years. This decrease is totally understandable if the accumulation of the damages and the rising uncertainty are taken into consideration.

The recent seismic activity has motivated Dutch authorities to some action, such as providing assistance to infrastructure and houses damaged by past events. Approximately 40,000 properties are considered at risk of damage by earthquakes and are being inspected by governmental authorities. Thousands of homes have developed cracks because of the quakes and plans are underway to shore up and reinforce the vast majority of them. Approximately 60,000 homes lie within the earthquake zone. The gas companies are dealing with about 6,000 damage claims.

Figure 4.1: (a) Damages on typical structures in the Groningen region due to the recent induced seismicity.

Figure 4.1: (b) Damages on typical structures in the Groningen region due to the recent induced seismicity.

5. THE AUGUST 16th, 2012, EARTHQUAKE NEAR HUIZINGE (GRONINGEN)

On the 16th of August, 2012, the strongest seismic event ever recorded took place near Huizinge in the Groningen region with magnitude Mw = 3.6 and focal depth approximately 3 km. Severe damage was caused to buildings and raised significant public concern. Maximum intensity of VI was detected in a limited region (< 4km) around the macroseismic epicenter. The exact distribution of the intensities experienced during the Huizinge event on 2012 is presented in the **Figure 5.1**. The maximum horizontal peak ground acceleration (PGA) measured is 85 cm/s^2, corresponding to a peak ground velocity of 3.45 cm/s for the record MID1-NS. Six accelerometer recordings with epicentric distance of 2 to 10 km were processed. The corresponding results, in terms of spectral acceleration and velocity (**Figure 5.3**), are being presented for the records which consist of two perpendicular components.

The characteristics of the main record, that yields the maximum PGA and PGV, are being investigated further. The aforementioned record comes from the station Middelstum-1 with epicentric distance in the order of 3 km. In the **Figure 5.4** the accelerogram is presented for the duration of its main pulses. Along with the accelerogram the corresponding wavelet plot is cited in an attempt to shed light in parameters such as the duration and number of the important cycles, the duration and effective period relation and the energy release in time domain.

From the acceleration spectra acquired from the records of the Huizinge event, it can be inferred that their period content is mainly in the range of 0 to 0.5 sec, while for period greater than 0.5 sec the spectral accelerations are decreasing rapidly. The maximum spectral acceleration was 217 cm/sec^2 corresponding to period 0.10 sec.

The wavelet analyses presented here have been conducted using Matlab software and employing the Morlet wavelet. From the several wavelets in the literature, the Morlet wavelet shown in **Figure5.2** is the most compatible with earthquake motions. It contains five cycles, with a shape quite similar to a ground motion record. The maximum period of interest in the results depicted in the scalograms is limited to 2-s period. In the graph given, the abscissa represents the real time, and the colors convey the match of the record at the relevant time slice with the pre-defined wavelet, or else the energy content, which is proportional to the level of amplification in terms of spectral acceleration. The energy content is produced as the multiplication of the amplitude and the frequency of the wavelet pieces summed up at each time step. The scalograms thus depict the fraction of the overall energy content (i.e. acceleration multiplied with time) of the record both in the time and frequency (period) domain.

From the wavelet analysis of the record coming from the Middelstum station for the NS direction (**Figure 5.4**), one strong pulse corresponding to period in the range of the 0.10 sec can be observed, highlighted with yellow color as indicated by the contour scale. This strong pulse is followed by limited pulses which are characterized of lower intensity and are falling in the same range of period.

Thus, it is plain to note that the period range of the energy release during the seismic quake perfectly matches with the natural period of the typical structures in the investigated area making them quite vulnerable to this kind of excitations.

In the study of Lange et al. (2011) **[10]** it is deemed that induced seismic events with magnitudes lower than 3.9 would not lead to significant structural damage to buildings and therefore the associated risk was considered acceptable until such theories were proven to be unrealistic by the end of 2012 that the strong ground motion took place.

The aforementioned seismic event increased the concern of the citizens and their confidence in the safety of their properties reached a low point. Before that event, it was established a feeling that the intensity of the earthquakes would not exceed a limit that could put the safety of the citizens of Groningen at stake, but this was not the case anymore. Updated seismic hazard analyses of the Groningen region set the upper limit of the magnitude that has the potential the hit the area in the future as M = 5 (Muntendam-Bos and de Waal, 2013) **[11]**, a level at which severe catastrophe cannot be excluded as a serious possibility since the majority of the building stock in the Netherlands is not expected to withstand strong seismic excitations.

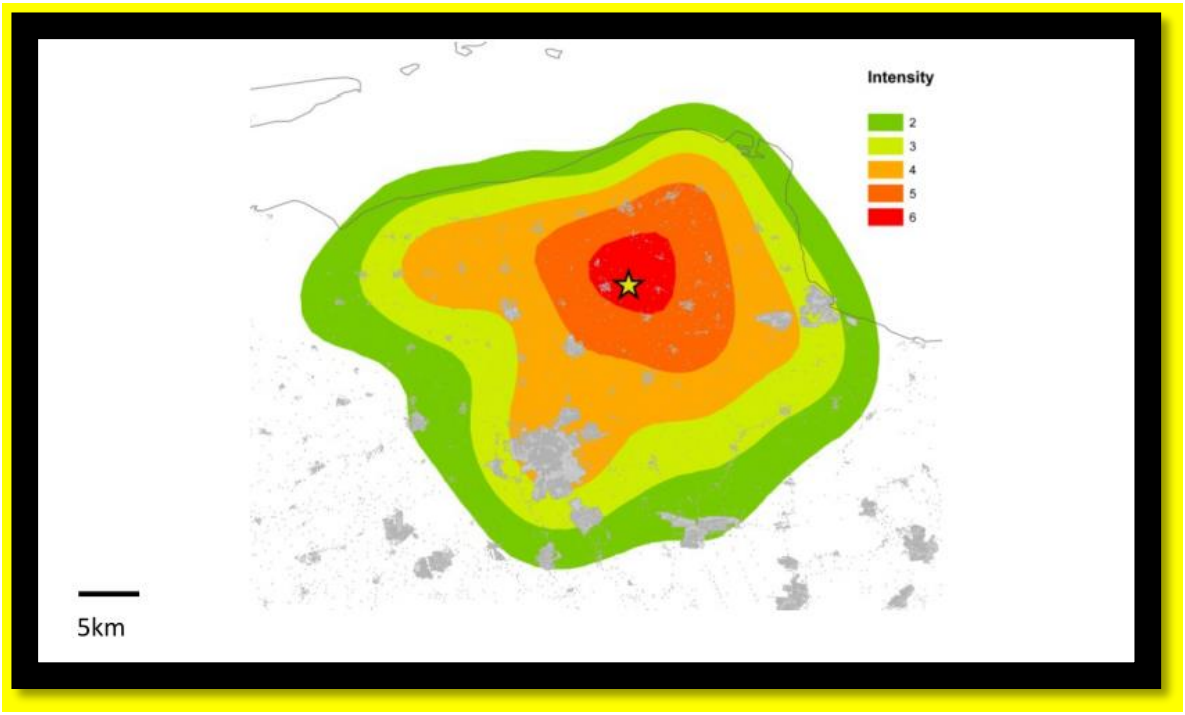

Figure 5.1: The exact distribution of the intensities (EMS98 intensity grades) experienced during the Huizinge event on 2012. The epicenter of the quake is marked with a star.

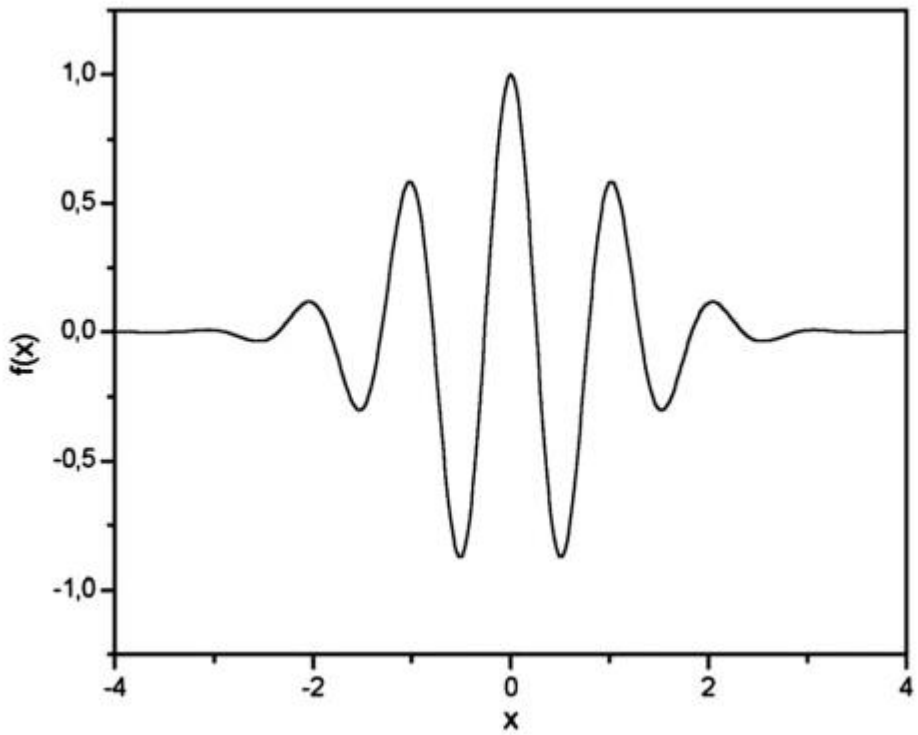

Figure 5.2: Morlet-type wavelet used in the analyses.

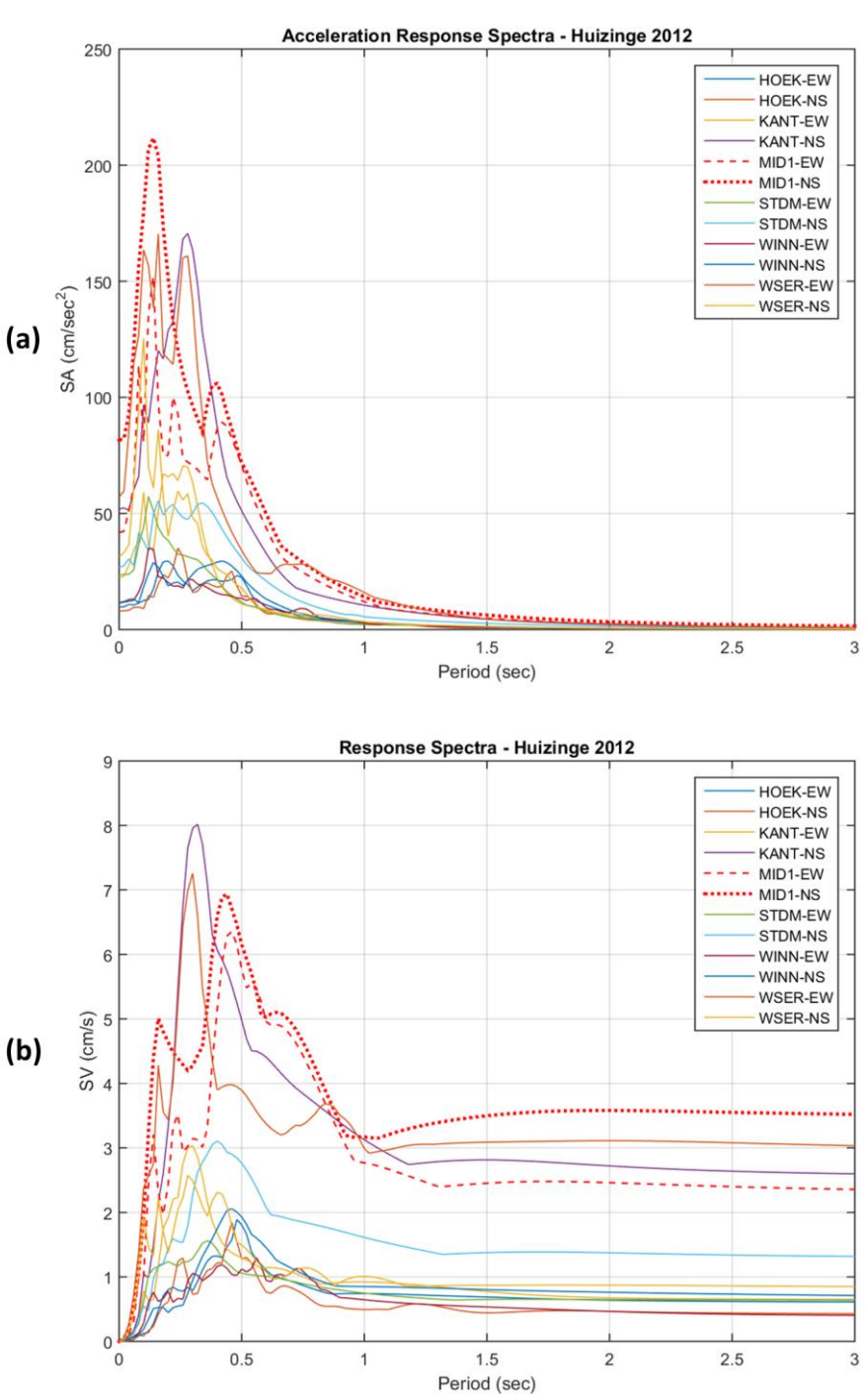

Figure 5.3: (a) The acceleration and **(b)** velocity response spectra coming from the records of the Huizinge event (2012) including their both component. The highest PGA corresponds to the record MID1-NS (dotted line).

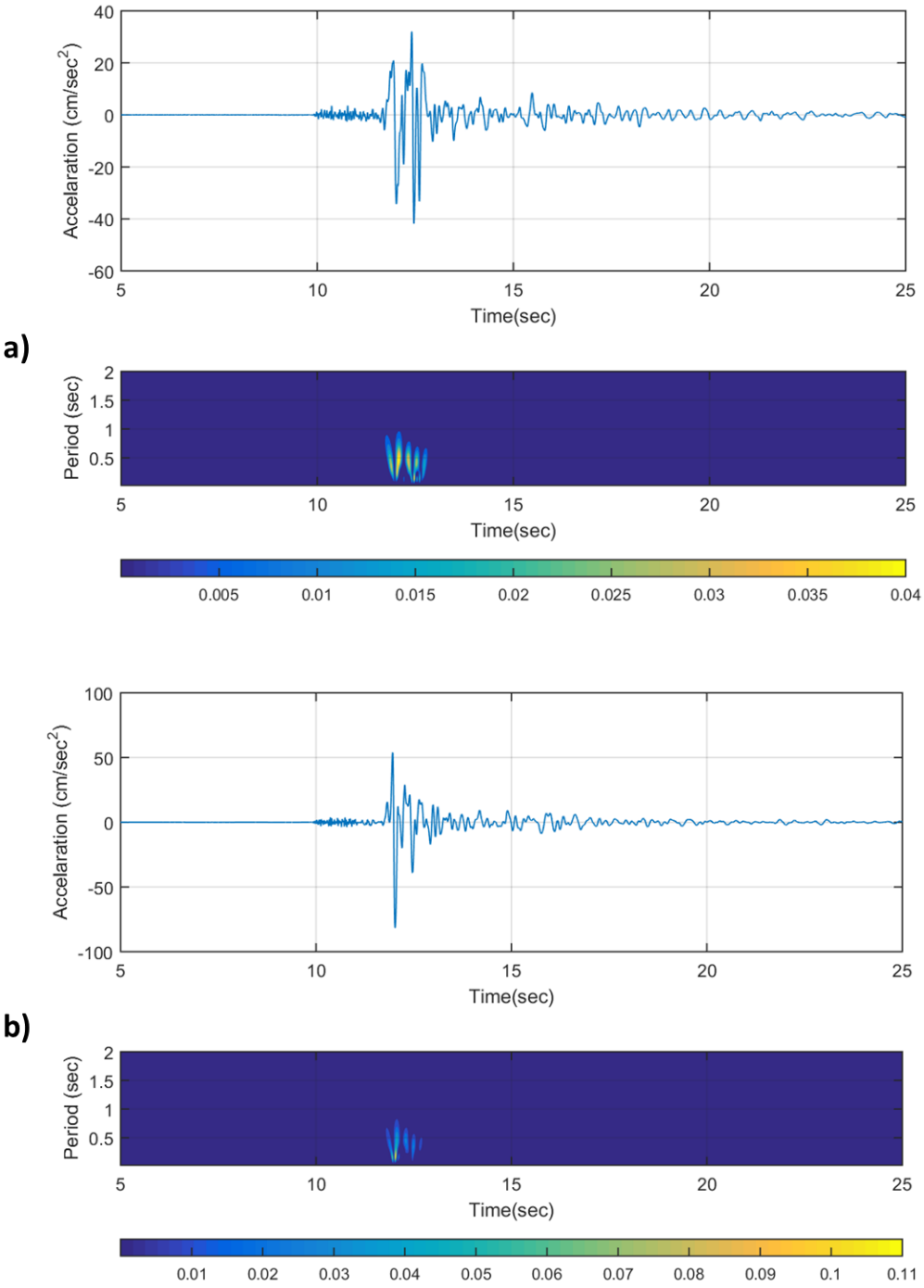
40
20
0
-20
-40
-60
Accelaration (cm/sec^2)
5
10
15
20
25
Time(sec)
2
1.5
1
0.5
Period (sec)
5
10
15
20
25
Time(sec)
0.005
0.01
0.015
0.02
0.025
0.03
0.035
0.04
100
50
0
-50
-100
Accelaration (cm/sec^2)
5
10
15
20
25
Time(sec)
2
1.5
1
0.5
Period (sec)
5
10
15
20
25
Time(sec)
0.01
0.02
0.03
0.04
0.05
0.06
0.07
0.08
0.09
0.1
0.11

a)

b)

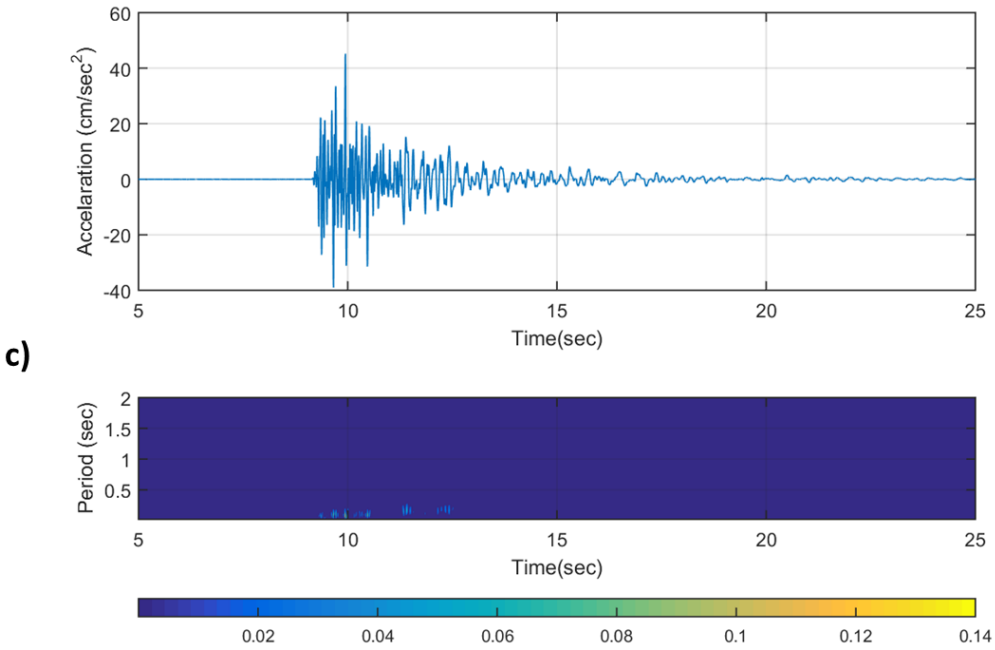

Figure 5.4: The main pulses of the accelerogram corresponding to the record MID1: **a)** EW, **b)** NS and **c)** VE (vertical) components in along size with its wavelet plot.

6. AVAILABLE EXPERIMENTS ON GRONINGEN-TYPE URM

Experiments sponsored by NAM (Nederlandse Aardolie Maatschappij) and conducted by EUCENTRE (Pavia, Italy) were carried out on full-scale wall specimens resembling the typical calcium-silicate unreinforced masonry walls that can be found in the Groningen region. Specifically, two wall specimens representing a slender and a squat wall, correspondingly, were investigated under in-plane cyclic shear-compression tests. Their characteristic and dimensions are given in the **Table 6.1**, and their experimental configurations are shown in the **Figure 6.1**. These two specimens were chosen to account for different types of wall that can be traced in real structures are characterized by flexure or shear dominated type of failure.

The test results presented herein are in terms of Horizontal Force – Drift/Horizontal Displacement (**Figure 6.2** and **Figure 6.3**). The time history of the horizontal displacement imposed during the experiment is given in the **Figure 6.5**. More detailed results can be found in the aforementioned studies **[12, 13]**. As it can be inferred from their pseudo-dynamic characteristics derived from the cyclic tests, their strength should be considered adequate to withstand the frequent but mostly weak seismic events that occur in the Groningen region. Specifically, some rough hand-calculations of the pseudo-dynamic response of the tested specimens will illustrate this assumption.

Taking into account the mass of the specimen for the squat wall (m =~13 ton) and the maximum spectral acceleration obtained from the Huizinge records (S_a =~ 2.2 m/sec^2). The derived base shear F_b is calculated as shown:

$$F_b = m * S_a = 28.6kN$$

Comparing the calculated base shear with the ultimate strength coming from the experimental results, that is F_{ult} =~ 60 kN, it can be easily inferred that the investigated specimen would yield an exclusively elastic behavior, since the seismic loading would only attain half of the prescribed strength of the specimen. The same calculations for the slender specimen yield similar results. These findings would lead to the hypothesis that the structures in the Groningen area should not be significantly affected by the seismic activity of the region and no damage would be expected under any circumstances. Nevertheless, the real case does not comply with this hypothesis since, as it was elucidated in previous chapters, distinctive damages took place during the recent years that the seismic activity is taking place.

Another intriguing finding of the experimental study of NAM came from the seismic analysis of a full-scale building test (**Figure 6.4**). The tested building was a representative case of the typical structures of the Groningen region and it was constructed following all the typical techniques utilized for the real houses. The aforementioned tests consisted of a suite of seismic excitations characterized by increasing intensity. In accordance with the NAM investigation, the very first slight damages in the tested building were observed for the seismic excitation that was corresponding to PGA in the order of 1.6 m/sec^2. In the **Figure 6.6** the illustration of the very first crack pattern that was formed in the tested structure is cited. This PGA value is twice as much as the recorded PGA value during the Huizinge event, which at the same time is the maximum ever recorded value for the studied region. This observation made it clear that the relatively strong seismic event of Huizinge on its own would not have the potential such an excessive damage as the one observed in the real case.

As a matter of fact, this led to the necessity to further investigate the response of the tested specimens not in the range of their ultimate strength but in numerous cycles of low range of loading which may finally play an important role in the overall response during a relatively stronger event. Specifically, a thorough investigation of the tests results pointed out that nonlinear phenomena take place for very limited value of top displacements. In the **Figure 6.2** and **Figure 6.3**, the first cycles of the conducted tests are presented for the squat wall – the results for the slender wall are equivalent and thus are not cited in this study. It can be noticed that the unloading branches do not follow the loading one, leading thus to a small amount of residual displacements even for quite low loading. This type of response leads to an assumption that the frequent quakes that strike the structures may produce a noticeable accumulation of displacements that has the potential to be more destructive when the relatively strong ground motion occurs. This assumption will be further investigated below.

In order to better understand the response of the Groningen-type URM to cyclic loads, focus on the load-deflection curves are presented here in **Figure 6.3**. In evaluating the load-deflection curves in earthquake engineering practice, it is more common to concentrate on the post-yield phase of the response. In the case presented here, however, the response in the very small cycles becomes important. It can be seen in **Figure 6.3(a)** that the very first cycles of the squat wall, there is a considerable amount

of hysteretic energy consumed, as well as residual displacements remained on the system. In this case, the top displacement is extremely small, in the range of 0.4 mm, translating into 0.01% top drift. The response becomes slightly different in **Figure 6.3(b)**, where the top drift ratio goes up to 0.015%, and a pinching type response is observed. The reason for this response may be either rocking of the specimen as it is, or failure of bed joints and partial rocking of the wall on one or multiple bed joints. In **Figure 6.3(c)**, on the other hand, ductility starts to build up leading to fatter hysteresis loops and obvious damage. When focused out to the overall response, as shown in **Figure 6.3(d)**, the response in the very first cycles gets invisible.

Zoom into the very first 3x3 cycles, as shown in **Figure 6.2 (left)**, provides insights regarding the extremely low amplitude response of the URM walls in question. The hysteresis loops of the first cycles is quite fat, leading to residual displacement and energy consumption, so damage, in the very beginning of their response. After analyzing several cycles in the experiments, the initial backbone curve suggested for the very low amplitudes can be seen in **Figure 6.2 (right)**. It should be noted that the main issue in this behavior, at the very beginning of the response, is the force drop when the cycles reverse. As opposed to bi-linear response, for instance, the constant is the displacement but not the load. This created practical problems in modeling these URM walls since none of the available and suitable models can consider a strength drop under constant displacement, since the hysteresis loops are mostly set for large deformations and the case is the increasing displacement under constant or slightly increasing/decreasing loads. More insights are provided on this issue in the rest of the paper.

In **Figure 6.2 (right)**, in line with the experimental results, there are two characteristic behaviors that need to be addressed in a suitable hysteresis loop, which are i) at the beginning of every unloading, there is a force drop of Force, and ii) the unloading stiffness is always smaller than the initial loading stiffness, thus the initial stiffness Ki is multiplied with a coefficient α, that is smaller than or equal to 1.0.

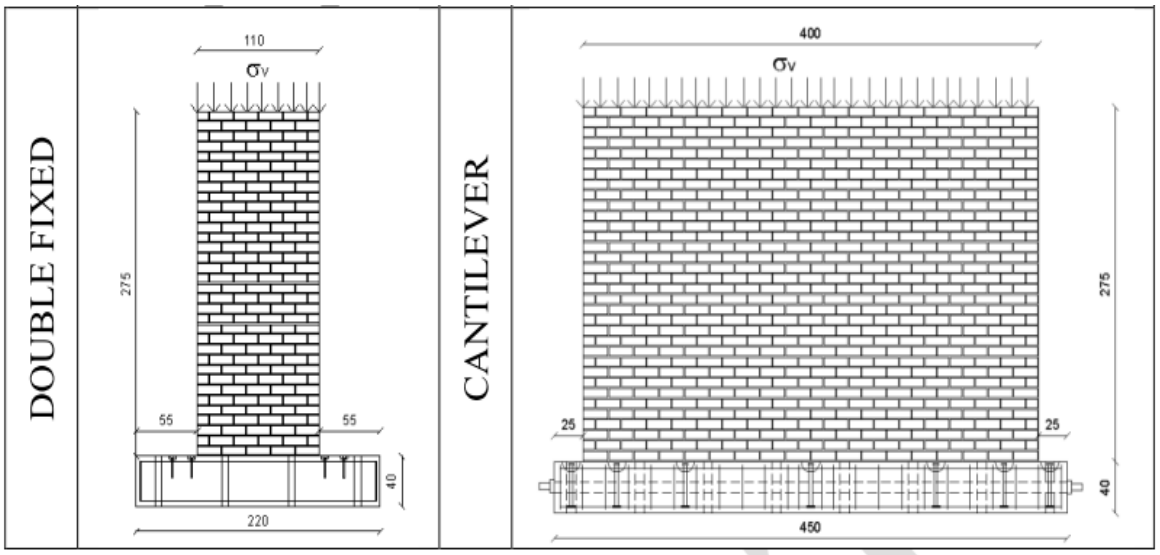

Figure 6.1: Experimental configurations considered, Slender Wall **(left)** and Squat Wall **(right) [12, 13]**).

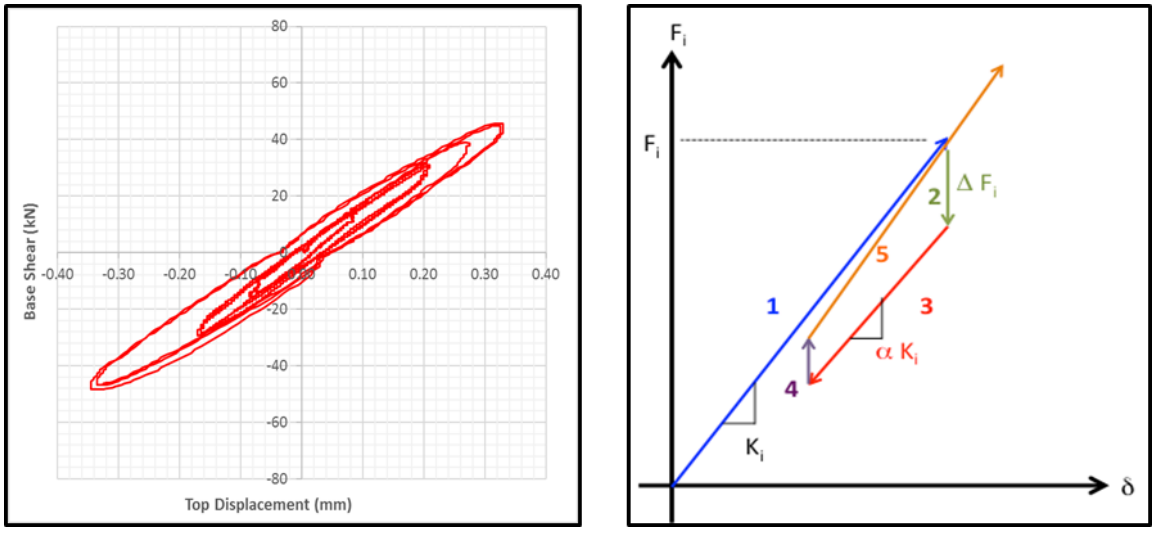

Figure 6.2: Focus on the experimental load deflection curve for the first 3x3 cycles **(left)** and an idealized hysteresis backbone **(right)**.

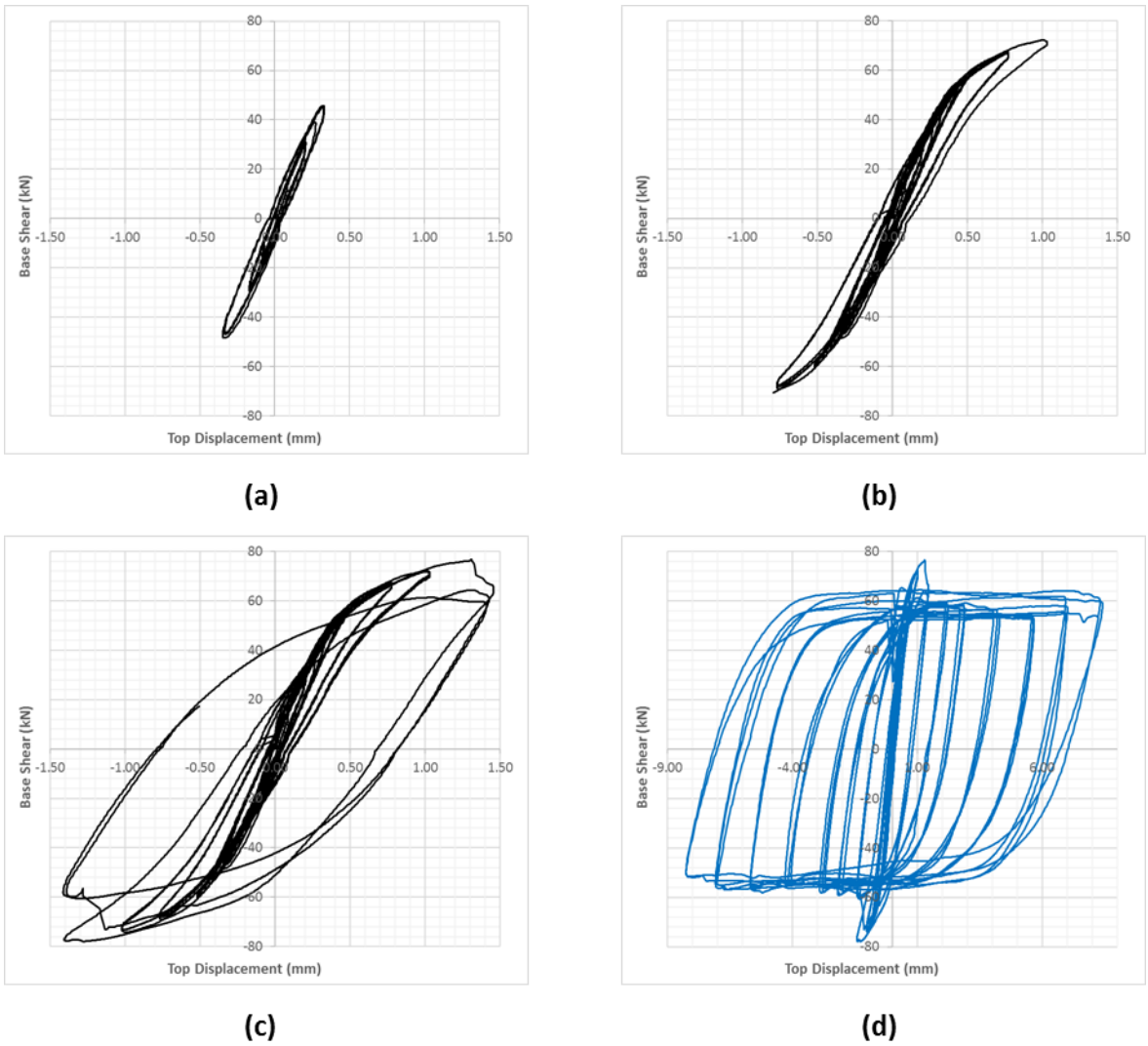

Figure 6.3: Experimental load deflection curve of the same EUCENTRE specimen (the squat wall specimen) focusing on different displacement ranges: **(a)** The first 3x3 cycles, up to 0.4mm top displacement, **(b)** The first 3x6 cycles up to 1mm top displacement, **(c)** The first 7x3 cycles up to 1.5mm top displacement, and **(d)** the full experimental hysteresis curve **[12, 13]**.

Figure 6.4: The specimen at the end of the construction.

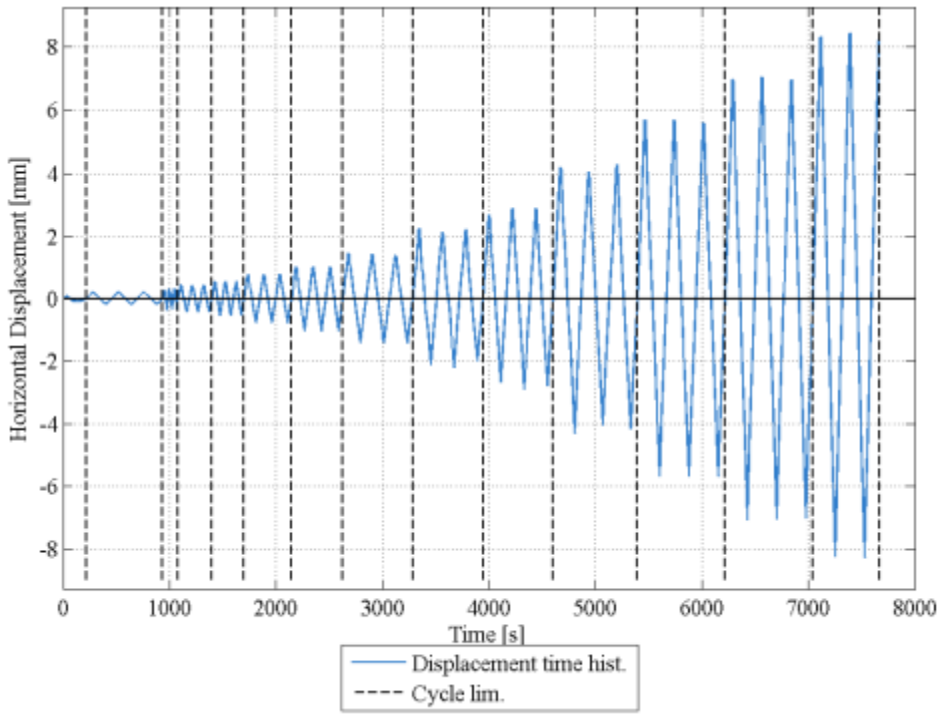

Figure 6.5: Time history of the horizontal displacement during the experiment.

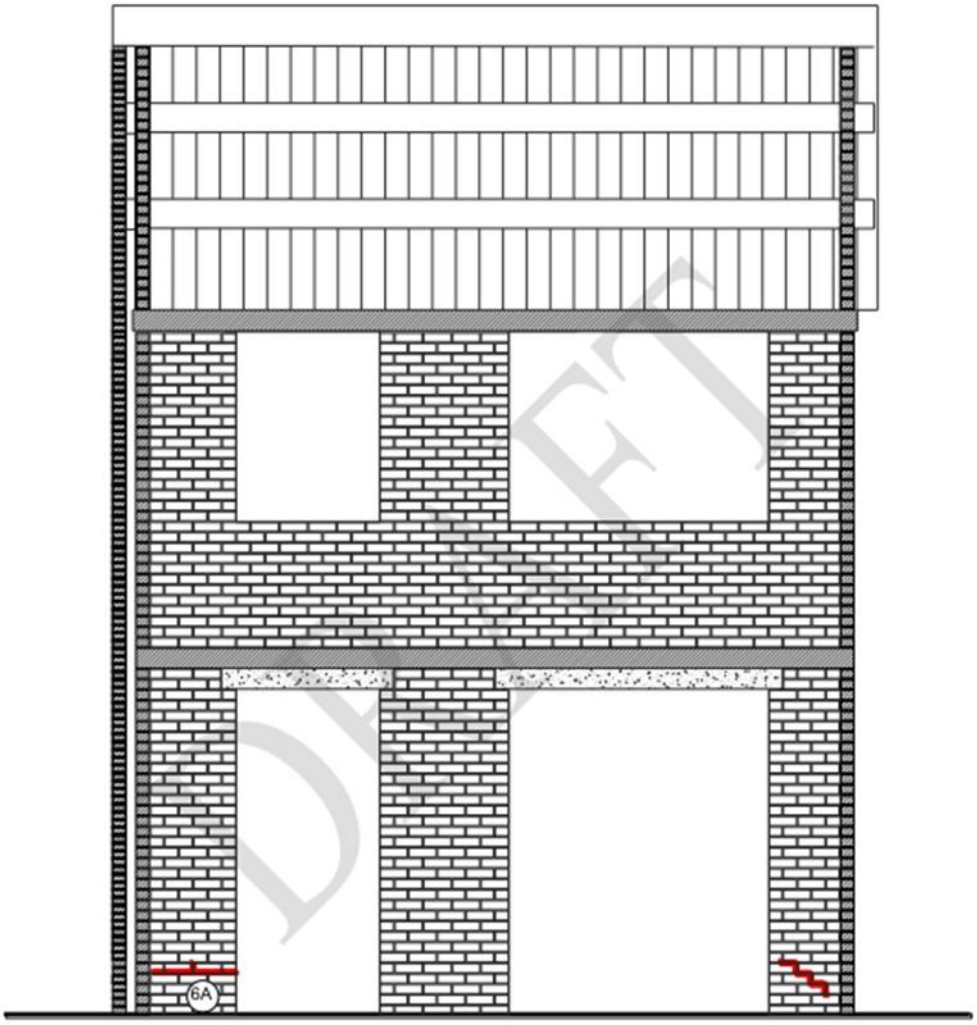

Figure 6.6: Section of the test-house - inner leaf - east side. Illustration of crack pattern (red lines) after the test #16, 100%_EQ2_160, PGA = 1.6 m/s^2.

Table 6.1: Characteristics and dimensions of the Tested Specimens.

Specimen	L (m)	t (m)	h (m)	σ_v (Mpa)	Boundary Conditions
Slender Wall	1.1	0.102	2.75	0.52	Double fixed
Squat Wall	4	0.102	2.75	0.3	Cantilever

7. EXERCISE WITH EXISTING HYSTERESIS LOOPS

7.1 Cyclic Loading

At this point, a simple numerical model was created in the SeismoStruct software (**Figure 7.1**) to simulate the response of the tested specimens for the very first cycles of the conducted experiments which seem to be of major importance. The Ramberg–Osgood **[14, 15]** constitutive model was applied on a link element, taking into consideration also the physical characteristics of the tested specimens, such as the mass, stiffness, and strength. The properties that were chosen for the arithmetical model are listed in the **Table 7.1**. The response of the utilized numerical model is presented in the **Figure 7.2**, comparing with the response of the corresponding specimen. Their comparison yields to a reasonable match in terms of horizontal force – top displacement response. Specifically, as it can be easily noticed, the loading branch that is reproduced with great accuracy. More importantly, the unloading and reloading branches are capturing the experimental response successfully. The non-linear phenomena, that are taking place even for low values of top displacement and were highlighted previously, are also simulated precisely.

Judging from these findings, the produced model will have the potential to capture the holistic response of the tested specimen with great accuracy. Apart from static analyses, the created model seems to be capable of simulating the response of the specimen also under cyclic excitation.

A projection of the herein study would be the utilization of the calibrated model in combination with the method suggested by I. E. Bal et al., 2010 **[16]** in order to model the response of a whole building and not being restricted in the simulation of the response of individual specimens.

7.2 Seismic Loading

The Seismic Database of the Groningen region can be found in the KNMI (Koninklijk Nederlands Meteorologisch Instituut) site. Unfortunately, not all the timehistories of the recorded events can be directly downloaded from the site. Due to this restriction, all the events for the year 2014 as recorded by the Middelstum station (BMD2) were chosen as a basis for the herein study. This station was selected because of its

proximity to the station that the highest PGA value of the 2012 Huizinge event was recorded. In **Figure 2.1(b)** the detailed distribution of the number of the earthquakes in combination with their magnitude is presented for the year 2014. This distribution was considered to be representative of the other years since it includes one record with magnitude 3, 18 records with magnitude between 1.5 and 3. In the **Figure 7.3** the whole timehistory of the 1-year bunch is shown.

The arithmetical model, that was calibrated against the experimental tests as discussed n previous chapters, was now utilized in an attempt to check the response of the simulated structure under seismic excitations. Emphasis is given on the validation of the assumption that the numerous but of lower intensity records do have the potential to affect the ultimate response of the structure while the strong ground motion will come. In order to do so the calibrated model was imposed in a series of time histories. Four different scenarios were chosen:

1) The Huizinge record of 2012 (PGA = 0.08 g) (**Figure 7.4**)

2) One year of all records that were recorded at the Middelstum region for in 2014 event (PGA = 0.07 g) followed by the Huizinge record of 2012

3) Five times the one-year of bunch that were recorded at the Middelstum region for in 2014 followed by the Huizinge record of 2012

4) Ten times the one-year of bunch that were recorded at the Middelstum region for in 2014 followed by the Huizinge record of 2012

Among the different records, which are included in the 1-year bunch, time spans of a few seconds were added of zero acceleration so that the structure would follow a free oscillation. This happened in an attempt to avoid any unrealistic attenuation that would occur if the records would be imposed the one exactly after the other.

The aforementioned scenarios were chosen this way in order to investigate the impact of the frequent but of low intensity quakes that strike the Groningen region in an annual basis to the stability of the structures when the strong event will follow.

The results of the different seismic scenarios are presented in terms of base shear versus top displacement and displacement over time (**Figures 7.5-8**).

As it can be claimed from the response obtained from the scenario #1 (**Figure 7.4**), the max top displacement reached up to 0.06 mm. The values coming from the

experimental results in respect to the yield displacement and collapse displacement are 0.45 mm and 8.2 mm correspondingly. Therefore, when the structure is being hit from the strong ground motion, under the assumption that its response will be as prescribed from the experimental results, no sign of failure or yielding would be expected. This deduction leads to the assumption that solely-acting the strongest ever recorded ground motion for the Groningen area does not have the potential to cause all the damages that are observed in the real case.

By using the calibrated Ramberg-Osgood model, and by applying several recursive seismic actions, it was found that the residual top displacement is approximately 0.05 mm after 2014 event, and it goes down to approximately 0.025 mm after the 2012 Huizinge event. Repetition of the 2014 event for 5 or 10 times does not alter this response.

This finding is not in line with the low-cycle fatigue tests with normal stresses, as reported in the literature. Additionally, after trying several hysteresis loops, the Ramberg-Osgood loop was found to be the most suitable for the very first cycles, however this model does not contain any cumulative damage parameter, leading thus to a non-realistic response where the system has tendency to re-center without accumulating damage. This is against the nature of URM material. It also should be mentioned that, even with the Ramber-Osgood parameters that fit the very first cycles, the post-yield response of the specimen was not modeled accurately.

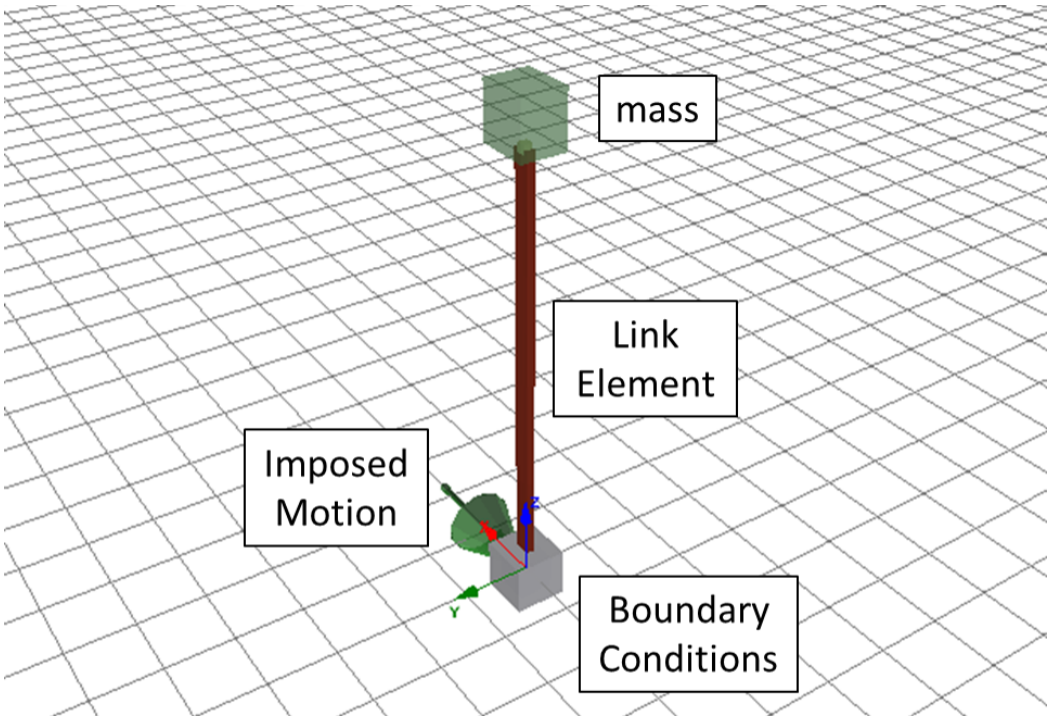

Figure 7.1: The numerical model created in the SeismoStruct software and its components.

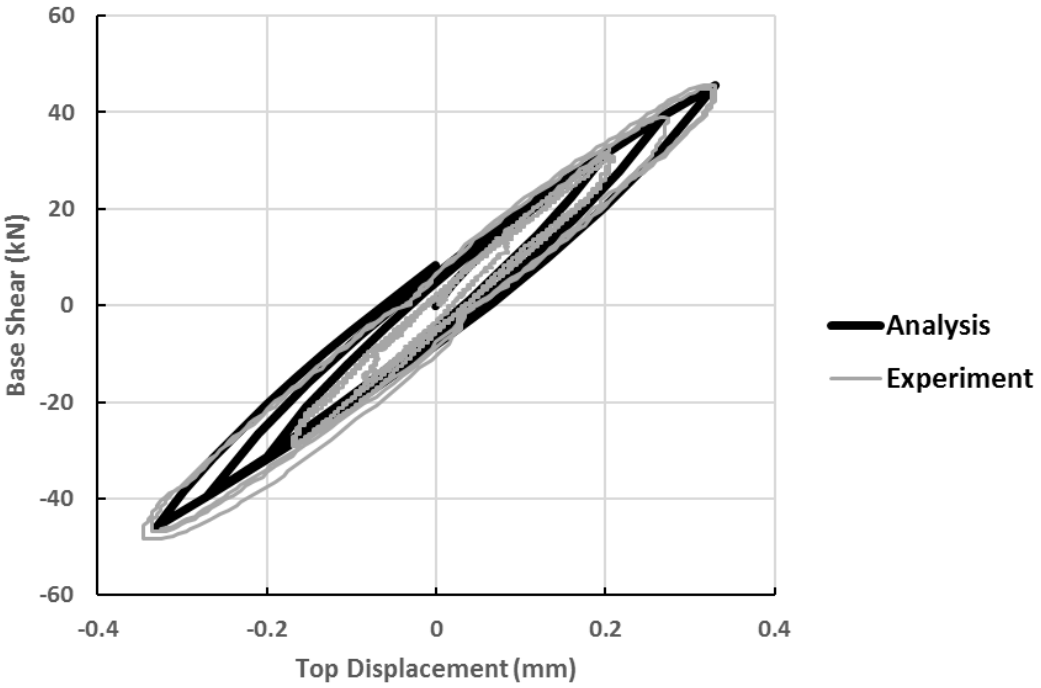

Figure 7.2: Calibration of the numerical model with the response of the tested specimen in terms of base shear versus top displacement for the first 3x3 cycles of the conducted experiment.

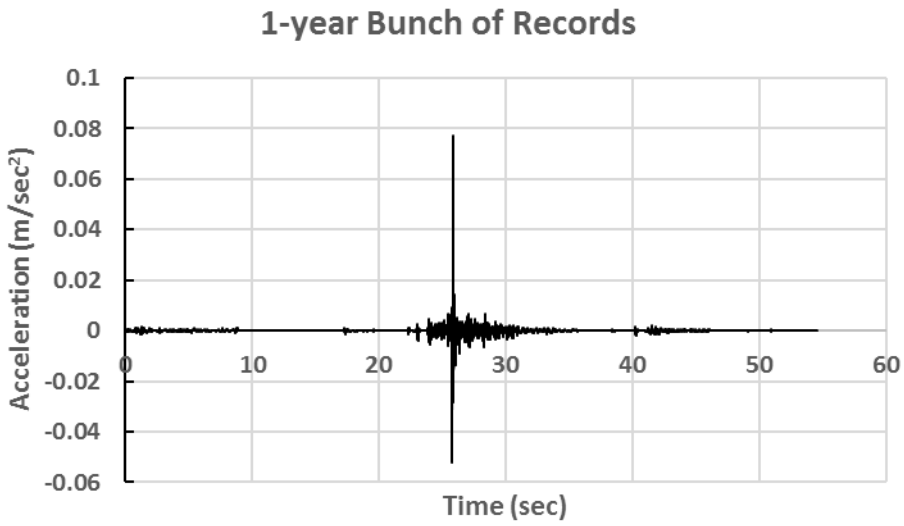

Figure 7.3: The acceleration timehistory that composes the 1-year bunch of records.

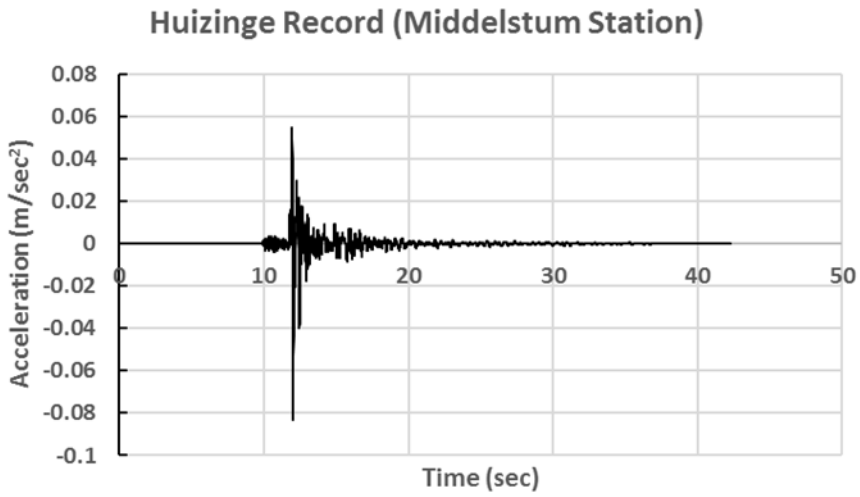

Figure 7.4: The acceleration timehistory obtained from the Huizinge record (2012), Middelstum station.

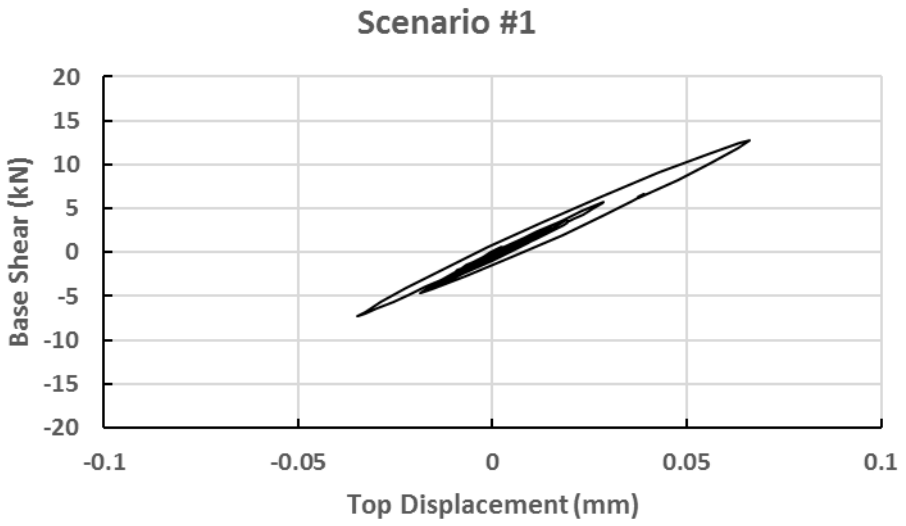

(a)

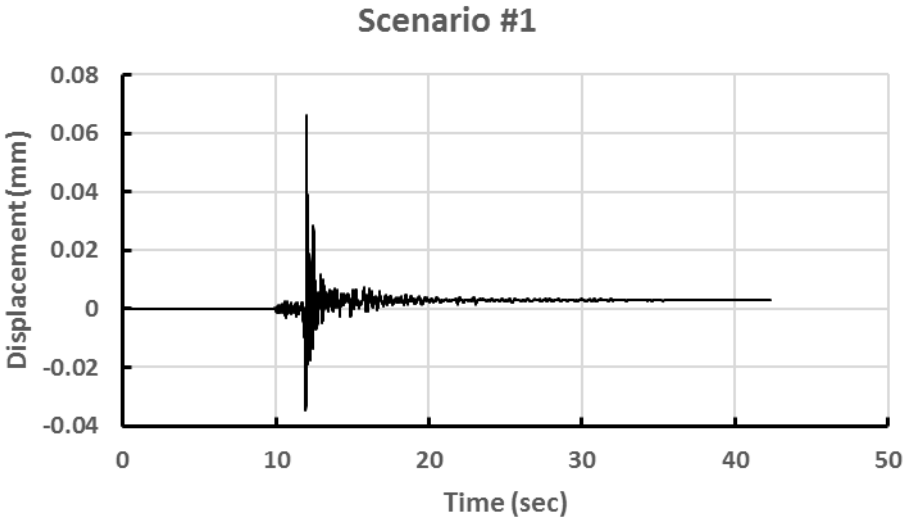

(b)

Figure 7.5: (a) Top displacement versus base shear and **(b)** the displacement over time for the time history of the squat specimen for scenario #1.

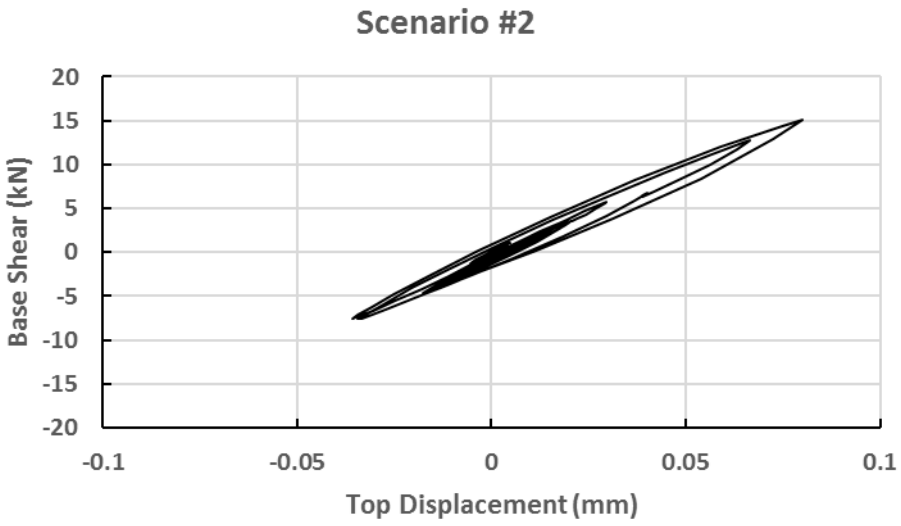

(a)

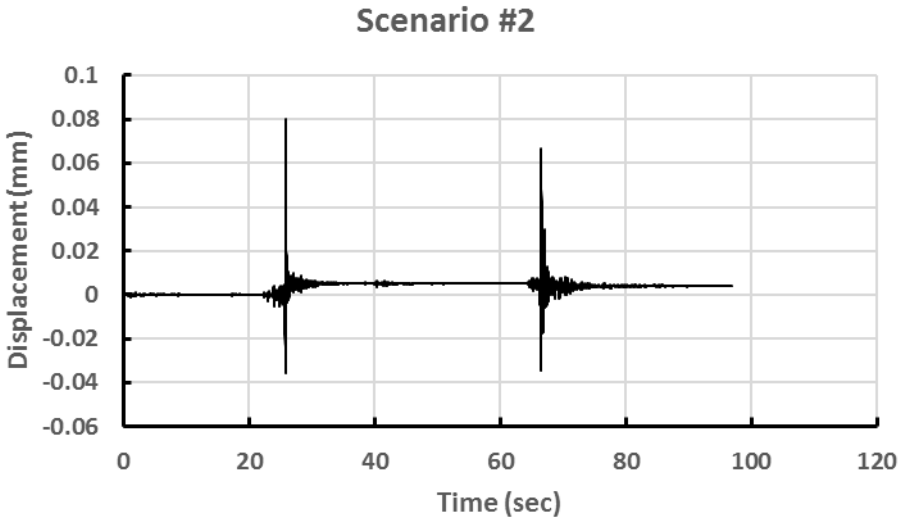

(b)

Figure 7.6: (a) Top displacement versus base shear and **(b)** the displacement over time for the time history of the squat specimen for scenario #2.

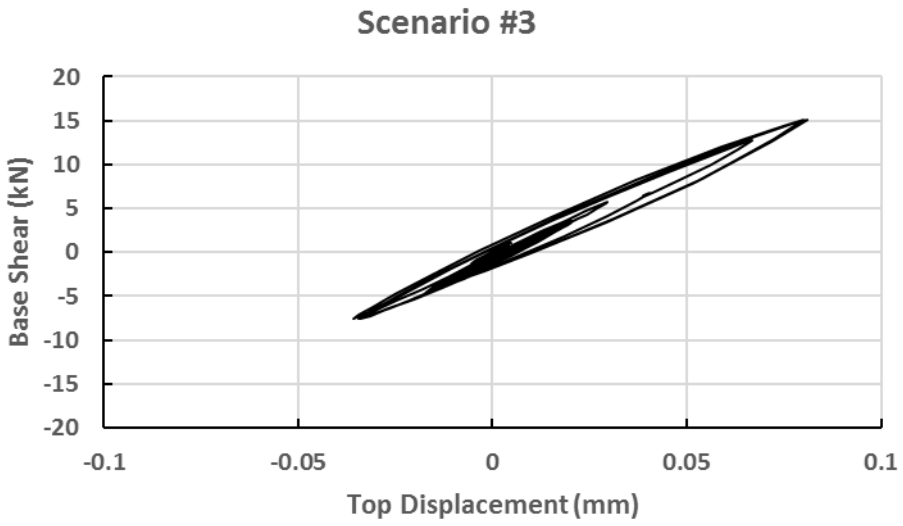

(a)

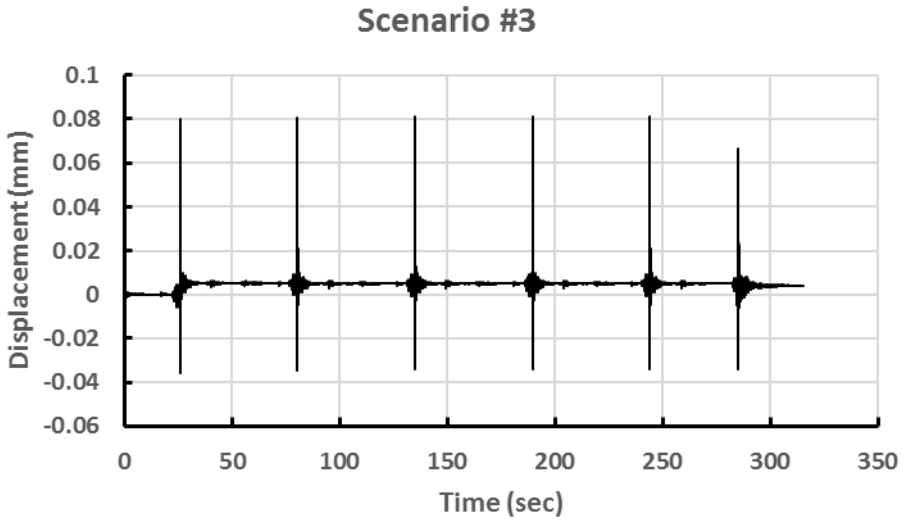

(b)

Figure 7.7: (a) Top displacement versus base shear and **(b)** the displacement over time for the time history of the squat specimen for scenario #3.

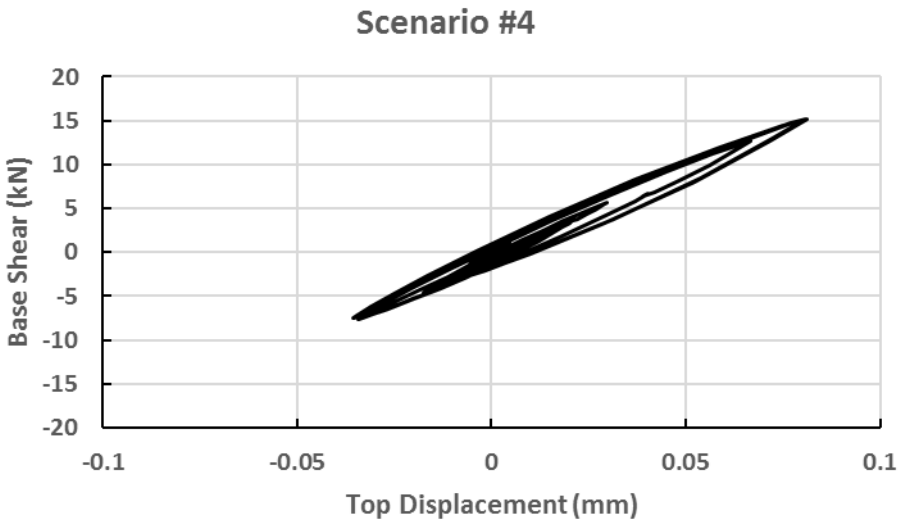

(a)

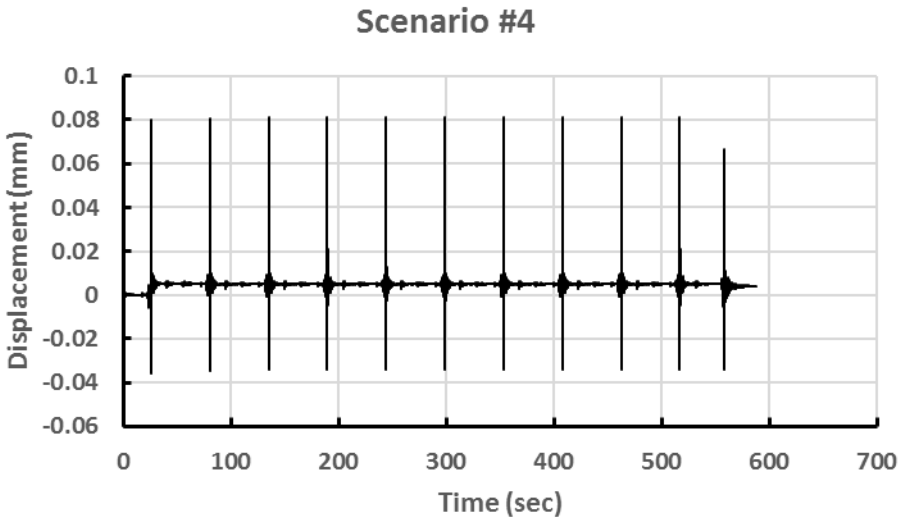

(b)

Figure 7.8: (a) Top displacement versus base shear and **(b)** the displacement over time for the time history of the squat specimen for scenario #4.

Table 7.1: The properties that were chosen for the calibration of the Ramberg–Osgood model in SeismoStruct software.

Yield Strength F_y	500
Yield Displacement	0.0025
Ramber Osgood Parameter	1.5
Convergence Limit	0.001

8. CONCLUSIONS

- Experimental evidence show that the response of the Groningen-type URM walls is quite different in the very first cycles then in the post-yield phase,
- The available hysteresis loops are designed to capture more accurately the post-yield phase, and thus are not suitable for the small amplitude cycles,
- The most well calibrated model was not able to present any cumulative damage, and even has tendency to re-center, contradicting the expectations and previous experimental findings under normal stress cases,
- There is a characteristic force drop in the small amplitude cycles in case of unloading, which cannot be modeled by using the widely available common hysteresis loops,
- A special hysteresis rule that represents not only the large displacement and the post-yield phase but also the very small amplitudes need to be developed.

[1] **Mulders, F**. (2003). Modelling of stress development and fault slip in and around a producing gas reservoir. Technical report, Delft University Press, Delft University, Netherlands.

[2] **McNamara, D. E., et al.** (2015), Reactivated faulting near Cushing, Oklahoma: Increased potential for a triggered earthquake in an area of United States strategic infrastructure, Geophys. Res. Lett., 42, 8328–8332, doi:10.1002/2015GL064669.

[3] Ground Water Protection Council and Interstate Oil and Gas Compact Commission. Potential Injection-Induced Seismicity Associated with Oil & Gas Development: A Primer on Technical and Regulatory Considerations Informing Risk Management and Mitigation. 2015. 141 pages.

[4] **Petersen, M. D. et al.** (2015), Incorporating Induced Seismicity in the 2014 United States National Seismic Hazards Models: Workshop and Sensitivity Studies, U. S. Geological Survey Open-File Report 2015-1070.

[5] **Roest, J. P. A. and Kuilman, W**.: Geomechanical Analysis of Small Earthquakes at the Eleveld gas Reservoir, in: Proc. Eurock '94, Balkema, Rotterdam, 573–580, 1994**.**

[6] **S. J. Bourne, S.J. Oates,** An activity rate model of seismicity induced by reservoir compaction and fault reactivation in the Groningen gas field 22 June, 2015.

[7] **Bierman, S., Kraaijeveld, F., Bourne, S.,** 2015. Regularised direct inversion to compaction in the Groningen reservoir using measurements from optical leveling campaigns. Technical Report. Shell Global Solutions International. Amsterdam. SeismoStruct v7.0 - User Manual.

[8] **Maqsud E Nazar, S.N. Sinha,** Behaviour of interlocking grouted brick masonry under low cycle fatigue loading, 14th International Brick and Block Masonry Conference (IB2MAC 2008), Sydney, Australia, 17-20 February 2008.

[9] **P. Ronca, A. Franchi & P. Crespi,** Structural failure of historic buildings: masonry fatigue tests for an interpretation model, Structural Analysis of Historical Constructions – Modena, Lourenço & Roca (eds), 2005.

[10] **de Lange, G., Oostrom, N. G. C. van, Dortland, S., Borsje, H., and de Richemont, S. A. J.:** Gebouwschade Loppersum, Deltaris 1202097-000, 84 pp., 2011 (in Dutch).

[11] **Muntendam-Bos, A. G. and de Waal, J. A.:** Reassessment of the probability of higher magnitude earthquakes in the Groningen gas field: technical report, February 2013.

[12] **Graziotti, F., Rossi, A., Mandirola, M., Penna, A., Magenes, G.** Experimental characterisation of calcium-silicate brick masonry for seismic assessment (2016) Brick and Block Masonry: Trends, Innovations and Challenges - Proceedings of the 16th International Brick and Block Masonry Conference, IBMAC 2016, pp. 1619-1628.

[13] **Graziotti F., Tomassetti U., Rossi A., Kallioras S., Mandirola M., Cenja E., Penna A., Magenes G. (2015):** Experimental campaign on cavity-wall

systems representative of the Groningen building stock. Report, EUC318/2015U, EUCENTRE, Pavia, Italy.

[14] **Ramberg W., Osgood W.R**. (1943): Description of Stress-Strain Curves by Three Parameters, National Advisory Committee on Aeronautics, Technical Note 902.

[15] SeismoStruct v7.0 - User Manual.

[16] **İhsan Engin Bal, Helen Crowley, Rui Pinho,** Displacement-based Earthquake Loss Assessment: Method Development and Application to Turkish Building Stock (2010).

CURRICULUM VITAE

Name Surname: Dimitrios Dais

Place and Date of Birth: Athens, 1991

E-Mail: dahs.dhmhtrhs@gmail.com

EDUCATION:

Diploma Degree.: 2015, National Technical University of Athens